Research Article

Full-duplex radio with two receivers for self-interference cancellation

Prafulla Deo[1], Dariush Mirshekar-Syahkal[2] ✉, Amit Mehta[3]

[1]Airbus Defence and Space, Anchorage Road, Portsmouth PO3 5PU, Hampshire, UK
[2]School of Computer Science & Electronic Engineering, University of Essex, Colchester CO4 3SQ, UK
[3]College of Engineering, Swansea University, Swansea SA1 8EN, UK
✉ E-mail: dariush@essex.ac.uk

Abstract: The design and implementation of a full-duplex radio system capable of real-time analogue self-interference cancellation at radio frequency and baseband stages are presented. The system consists of a dual-patch three-port orthogonally linear polarised antenna system (without a circulator/duplexer), a homodyne dual receiver, and a differential amplifier at the baseband. The interference outputs from the two receivers are equalised using a fixed attenuator and when they are passed through the differential amplifier at the baseband they are effectively cancelled. For the system reported the antenna system provides 45.1 dB isolation between transmit and receive ports over 60 MHz bandwidth centred at the operating frequency of 3.2 GHz. Interference cancellation achieved by the differential amplifier at the baseband reduces the total self-interference to 81.5 dB minimum at −5.6 dBm transmit power. Using the proposed system, the recovery of two different types of baseband signals in real time is demonstrated while the surrounding is multipath enabled. Since the self-interference at baseband is removed by the differential amplifier instead of a complex digital signal processing unit, it makes the proposed system suitable for broad-band millimetre-wave full-duplex transceivers where the use of analogue/digital converter is not an option.

1 Introduction

Due to the rapid surge in the amount of data traffic over the wireless networks, one of the key challenges for the current and next-generation wireless systems is efficient utilisation of the available spectrum to attain higher data rates. Full-duplex (FD) systems, where communication in both directions is carried out over the same frequency channel simultaneously, have been evolving as a promising mechanism with the potential to double the data throughput when compared to a half-duplex configuration utilising the same frequency channel [1]. The main limitation in realising a FD system is the presence of strong self-interference (SI) signal from the transmit antenna towards the receive antenna within the same transceiver system. In recent times, the problem of SI cancellation in FD systems has been addressed using different techniques [1–7].

The required amount of SI cancellation depends on the transmitter power and transmitted signal bandwidth. Typically, an SI cancellation of 60–110 dB is required for realising an FD system. To attain this amount of suppression, the SI cancellation mechanism is implemented in multiple stages across the FD system, leading to high design complexity. Normally, the SI cancellation approaches use a combination of passive suppression, active cancellation, and digital baseband cancellation.

In passive suppression techniques, the SI signal is mitigated by careful design of transmit and receive antenna structures where antenna polarisation, antenna separation, and antenna placement as well as antenna directionality are exploited [8–10]. In active cancellation, the SI is alleviated by subtracting a copy of the transmitted signal from the received signal [3, 11, 12]. In digital cancellation [13–15], an accurate copy of the SI signal is created using an effective estimate of the SI channel and transceiver impairments.

Usually, an attempt is made to cancel most of the SI in the antenna system in order to lessen the complexity of SI cancellation in the rest of the stages. A common way to obtain further SI cancellation is to pass a copy of the transmitted (Tx) signal through variable delay lines and attenuators and subtract it from the SI signal arrived at the receiver input [3]. If the variable devices in the active cancellation are dynamically controlled and the antennas are properly arranged, a large overall cancellation of up to 60 dB can be achieved [3]. The approach is promising; however, to make the system work, the attenuators and delay lines need to be reprogrammed continuously to compensate for the multipath reflections. This is a non-trivial task and would require a significant investment in hardware and software resources.

In this paper, a new FD system based on a dual-receiver design is proposed which uses a dual-antenna system and a copy of the transmitted signal for SI suppression to 81.5 dB. The dual-antenna structure, benefitting from orthogonal polarisation, significantly reduces the SI mainly due to mutual coupling between transmitter and receiver. Following the dual receiver, a differential device – in this case a differential amplifier (DA) – at the baseband is employed to effectively remove the remaining SI in real time in order to achieve additional isolation. In the proposed system, the SI at baseband is removed by the DA instead of a complex digital signal processing unit. This property makes the system suitable for broad-band millimetre-wave (mm-wave) FD transceivers where the use of analogue/digital (A/D) converter is not an option. As well, the system offers other advantages as will be mentioned later. Two examples of signal recovery with the proposed system are also presented.

2 Proposed SI cancellation technique

The SI cancellation proposed in this paper is based on a dual-receiver employing three antennas and a DA. The transreceiver block diagram is illustrated in Fig. 1. It does not have the shortcoming and complexity of the system in [3] as alluded in Section 1, since the residual interferences after the antenna system detected by the two receivers are subtracted at the baseband by the DA.

In the proposed system, the antennas in the two receivers have the polarisation orthogonal to that of the transmitter antenna. In this case, the polarisations have been chosen to be linear, but left and right circular polarisations can be used too. After equalisation using a fixed attenuator (in Rx1), the outputs from the two receivers are subtracted in the DA to generate the received signal.
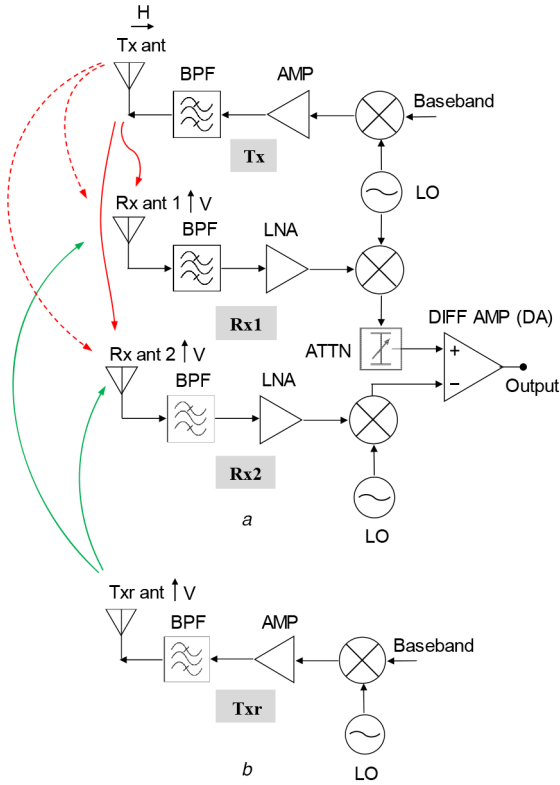
Fig. 1

(a) Proposed direct conversion FD radio system with its LO shared between Rx1, Rx2 and Tx, and *(b)* Remote data transmitter (Txr) with its own separate LO. H (horizontal) and V (vertical) denoting the polarisations of transmitting and receiving antennas. Green arrows denoting the signal of interest whereas red arrows indicating the near-field (solid line) and self-multipath interference signal (dotted line)
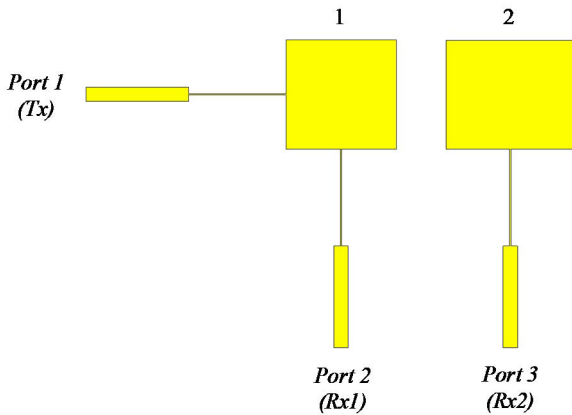
Fig. 2 *Three-port dual-polarised dual-patch antenna. Antenna 1 used for transmission (port 1) and providing a copy of transmitted signal to the dual receiver. Antennas 1 and 2 are connected to the dual receiver through ports 2 and 3*

In the FD radio system shown in Fig. 1, Rx1 (the first receiver) is homodyne and has an antenna closest to the Tx (the transmitter) antenna. Rx2 (the second receiver) is also homodyne and has an antenna located further away from the Tx antenna but only slightly away (much less than a wavelength) from the Rx1 antenna. Both receivers Rx1 and Rx2 share the same local oscillator with the transmitter Tx. In the experimental system the antenna system uses two patch antennas and Tx and Rx1 share the same patch antenna, as shown in Fig. 2.

Due to the close proximity of Rx1 to Tx, Rx1 essentially detects the near-field SI as well as the self-multipath SI generated by surrounding objects reflecting any of Tx signal. Due to higher isolation of Rx2 from Tx, it picks up signal (received data) from remote Txr as well as near-field and self-multipath SI. Considering Rx1 and Rx2 antennas are well correlated, the SI signal in Rx2 is

almost the replica of SI in Rx1 to within a multiplying factor (correctable by a fixed attenuator in Rx1). Therefore, they are expected to be significantly cancelled through the DA (Fig. 1).

There are three main advantages with the proposed system as for instance compared with that in [3]. Firstly, it can accomplish an effective cancellation of all the SIs with using only antenna isolation and an analogue cancellation stage. Secondly, due to the close proximity of antennas of Rx1 and Rx2, the proposed system is capable of cancelling self-multipath reflections in real time without requiring a phase shifter. Thirdly, it does not need phase shifters for adjustment of SI in narrow-band operation. Fourthly, the attenuator in the system (Fig. 1) is of a fixed value. Furthermore, the system is readily scalable to mm-wave frequencies where the use of A/D for wide basebands (a few GHz) is a major problem (as noted earlier).

In the following sections, details of the designs of the three-port dual-patch antenna, the FD system, and the experimental results are presented and discussed.

2.1 Three-port dual-polarised dual-patch antenna

The dual-patch three-port orthogonally polarised square microstrip patch antenna system used in this work is shown in Fig. 2. The FR-4 substrate with $\varepsilon = 4.2$ and a thickness of $h = 1.6$ mm was used for antenna implementation. The antenna system was designed for the centre frequency 3.2 GHz (of free space wavelength $\lambda_0 = 93.75$ mm) and its performance was simulated using CST Studio Suite software [16]. Port 1 is used as the transmitting port, and ports 2 and 3 are the receiver ports. The resonant lengths of both patches are the same and are equal to 21.5 mm in order to have the same transmit and receive operating frequency of 3.2 GHz. When port 1 is excited, the Tx antenna generates the horizontally polarised radiation, whereas ports 2 and 3 receive the vertically polarised radiation. Thus, there would be good intrinsic isolation between the transmitter and receiver port owing to the orthogonal polarisations between the transmitter and receiver ports. While the width of antenna 1 is the same as its length, the width of antenna 2 connecting to port 3 is chosen to be 25 mm, slightly larger than the width of antenna 1 terminated to port 1. In this case, antenna 2 is detuned for the horizontal polarisation (cross-polarisation) of radiation associated with Tx at 3.2 GHz; therefore, even higher isolation between Tx and Rx2 becomes achievable. Indeed, increasing this isolation using a more complex technique like electromagnetic band gap implementation will be rewarding as it decreases the SI in Rx2 leading to higher signal-to-interference-plus-noise ratio at the DA output.

The centre-to-centre distance between the two patch antennas is 33 mm (about $0.35\lambda_0$). The edge-to-edge separation between antennas 1 and 2 is 9.75 mm (about $0.1\lambda_0$). The small distance between the antennas would ensure that the desired signals arriving at the antennas are nearly of the same magnitude and phase at ports 2 and 3. This small distance is also advantageous since any signal from Tx reflected back by the surrounding objects (self-multipath interference) arriving on both patches would be nearly identical and hence they can be removed in the baseband stage. Ideally, the two antennas need to be co-located to have the above said effects to the full.

As seen in Fig. 3, where the measurement and simulation results are compared, the measured return losses at 3.2 GHz for ports 1, 2 and 3 are 25.6, 22.6 and 17.8 dB, respectively. The -10 dB impedance bandwidth is 60 MHz ($\simeq 2\%$) covering the frequency range of 3.17–3.23 GHz. The inter-port isolation between ports 1 and 2 is $S_{21} \simeq 31.8$ dB and between ports 1 and 3 is $S_{31} \simeq 45.1$ dB both at 3.2 GHz as shown in Fig. 4. However, as seen in Fig. 4, over the -10 dB impedance bandwidth of 60 MHz, S_{21} and S_{31} vary with frequency, but their difference over the band remains almost constant and about 13.3 dB. This is an important advantage, since if the difference is frequency dependent, the attenuator in Fig. 1a needs to compensate for the frequency variation of the difference in order to achieve good SI cancellation using the DA. Also in Fig. 4, where the phases of S_{21} and S_{31} are depicted, the difference between their unwrapped phases is about 360° within the band for the proposed antenna system. However,
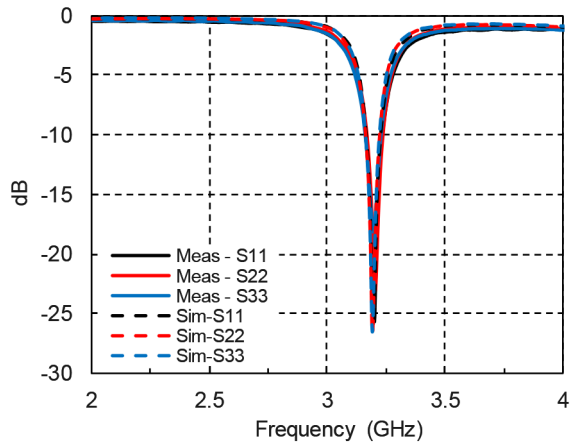
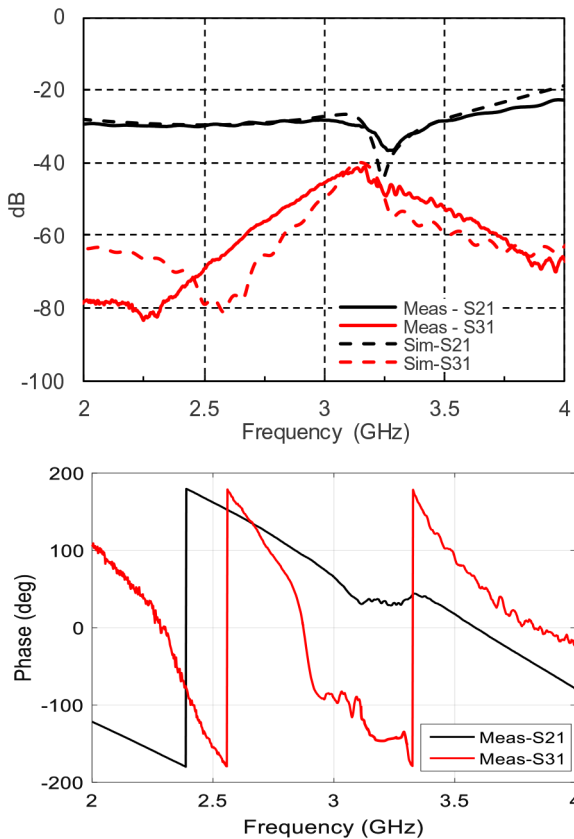**Fig. 3** *Reflection coefficients for the two-patch three-port antenna*

Fig. 4 *Isolations (mag. and phase) between ports for the two-patch three-port antenna system*

Fig. 5 *Three-port dual-polarised dual-patch antenna radiation patterns at 3.2 GHz for different ports*

a

b
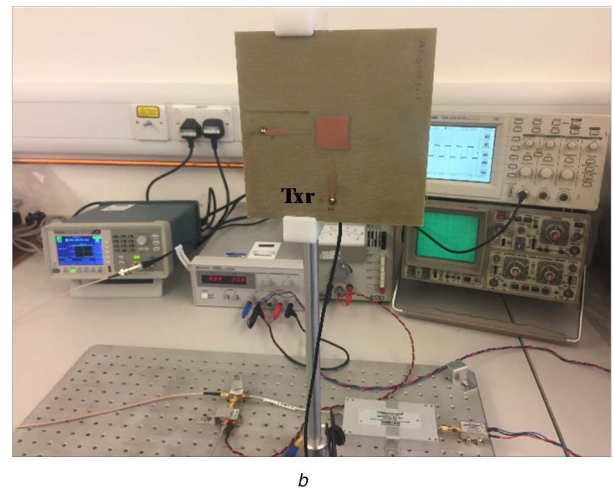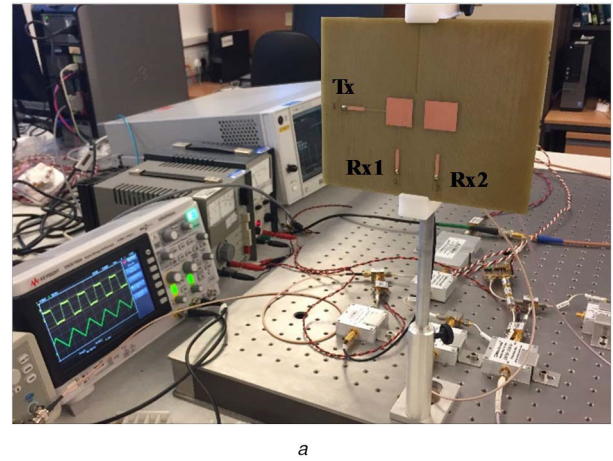
Fig. 6 *Experimental setup for*
(a) FD system, *(b)* Remote data transmitter (Txr)

since the fractional bandwidth is small (2%), this large radio frequency (RF) phase difference causes only minor misalignment between baseband SIs detected by the two receivers, arriving at the DA inputs. Fig. 5 shows the radiation patterns at 3.2 GHz for excitation of each port. The antenna system has a maximum gain of 4.8, 5.1 and 5.3 dB for excitation of ports 1, 2 and 3, respectively. Half-power beamwidths associated with ports 1, 2 and 3 are 103°, 66.4°, and 70.3°, respectively.

In the next section, the performance of the dual-receiver system including the dual-patch antenna system (already presented in this section) and the DA at the baseband stage for the SI cancellation is presented.

2.2 SI cancellation performance

Based on the proposed FD radio architecture (Fig. 1), a full working system operating at the centre frequency 3.2 GHz has been developed (Fig. 6). The antenna system is specified, designed and tested, as explained in the previous section. The other
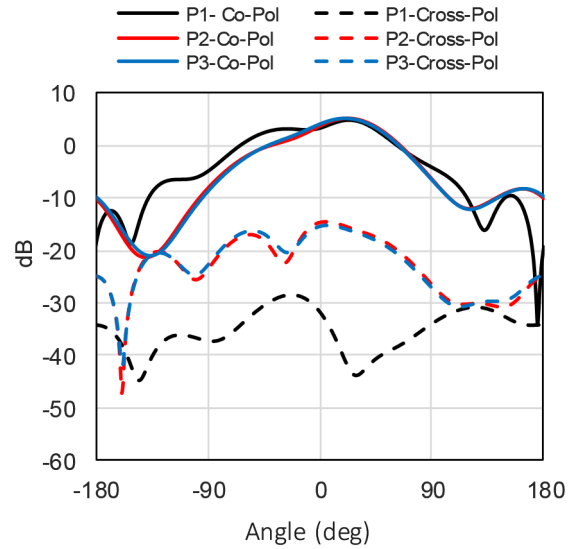
subsystems used include 3100–3300 MHz bandpass filters (ZAFBP-3200-S+), 600–8000 MHz low-noise amplifiers (ZX60-83LN-S+), 20–4000 MHz driver amplifiers (ZX60-4016E-S+), 2300–8000 MHz mixers (ZX05-83-s+), 0–4000 MHz variable attenuator (ZX76-15R5A-x) and 0–12,000 MHz attenuator (FW-x), all by mini-circuits. In this dual-receiver system the proposed analogue cancellation circuit in the baseband uses a commercially available DA known as analogue devices AD524ADZ. It is not very broadband and has an inadequate transient response, but it is sufficient to demonstrate the principals.
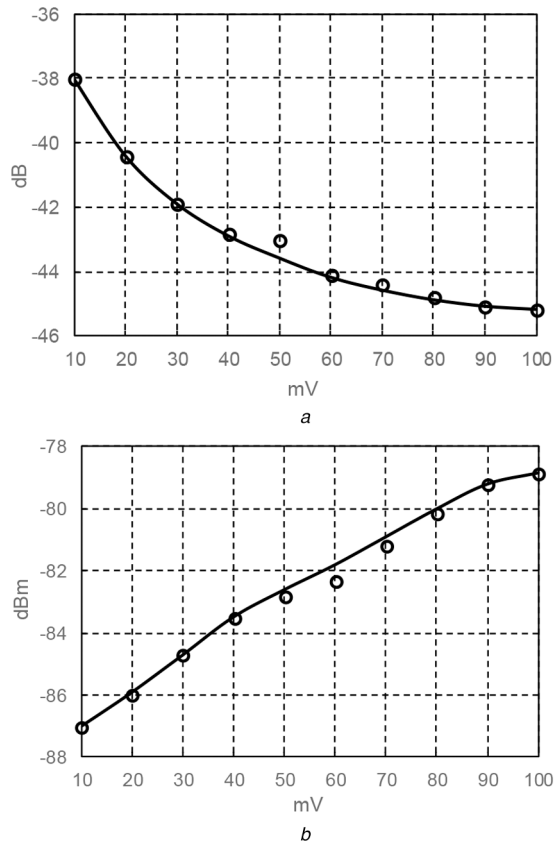
Fig. 7

(a) SI rejection, *(b)* SI level of the proposed FD system at the DA output for the modulating signal amplitude between 10 and 100 mV

To check the capability of the system, first both Txr (remote transmitter transmitting data) and Tx shown in Fig. 1 were shut down and the noise floor at the output of the receiver (output of the DA) was measured to be −95.1 dBm.

Then Txr whose antenna located at 1.9 m from the receiver antennas was switched on; in this case, there was no modulation imposed on the carrier [3.2 GHz − i.e. the frequency of the local oscillator (LO) tuned to 3.2 GHz]. Power measured at the input of Txr antenna was −5.8 dBm. Powers received at the output of antennas at Rx1 and Rx2 were measured to be around −48.5 dBm which is in agreement (within a few dBs) with the value from the link budget equation considering the gains of the antennas are around 5 dB (Section 2.1). In this case the noise level measured at the receiver output (DA output) was −94.7 dBm. This is 0.4 dBm higher than the receiver noise floor and could account for noise from Txr carrier signal.

Next, Txr was shut down and Tx was switched on with no modulation imposed on its carrier (3.2 GHz). The power at the input of the Tx antenna (port 1) was recorded to be −5.6 dBm (which is close to that at the Txr antenna in the previous experiment). Rx1 connected to port 2 of antenna 1 is used to obtain the copy of the transmitted signal from Tx. The power at port 2 due to the SI (near-field and self-multipath interference) was measured to be around −36.5 dBm. Therefore, the isolation at port 2 is around 30.9 dB, which agrees with the S21 measurement of the antenna (31.8 dB, Fig. 4). Rx2 connected to antenna 2 (port 3) receives a weaker copy of the transmitted signal plus the self-multipath interference. Owing to the orthogonal polarisation between ports 1 and 3 and the choice of the edge-to-edge separation of the two antennas (Fig. 2), the interference power from ports 1 to 3 together with the self-multipath interference received at port 3 was around −50.9 dBm, being as expected lower than the previous case. The isolation of 45.3 dB between Rx2 and Tx agrees with the measured results of S31 (45.1 dB, Fig. 4) for antenna 2. In this test the noise floor at the receiver output was measured to be around −95.8 dBm similar to that when Tx was off.

Since the two SIs received by Rx1 and Rx2 are almost scaled copies, adjustment of the attenuator at the output of Rx1 by about 14.4 dB (50.9–36.5 dBm) would virtually eliminate the interfering baseband signal due to Tx at the output of the DA. Further, as Rx2 has 14.4 dB lower SI, the baseband signal (data) received from Txr can be imagined as 14.4 dB stronger in Rx2 and hence would become readily detectable. Therefore, as mentioned in Section 2.1, increasing the isolation of the second antenna would favour the detectability of the desired signal. Due to 0.5 dB attenuation resolution of the variable attenuator (ZX76-15R5A-x) used, the attenuation in the Rx1 channel had to be set at 14.5 dB. The attenuator is broadband (0–4000 MHz), and over the 60 MHz baseband (set by the antenna system bandwidth as mentioned previously in Section 2.1) it did not present a measureable phase shift in Rx1 channel to upset the SI power balance achieved in the two channels and hence, had a little observable effect on the SI cancellation by the DA circuit (Fig. 1). It is interesting to note that the difference in the isolations of Rx1 and Rx2 antennas from Tx is expected to be 13.3 dB over the 60 MHz bandwidth as pointed out earlier in Section 2.1. Although 13.3 dB should be the required attenuation at the Rx1 path before the DA, the actual attenuator needed was 14.4 dB. Further investigation revealed that the difference (14.4 dB−13.3 dB = 1.1 dB) can be attributed to unmatched magnitude responses in the operation of the components (filter, amplifier, and mixer) in the two receivers over the small fractional bandwidth of 2%.

To investigate the SI rejection and generated SI level of the proposed FD system at its DA output when Tx delivers a baseband signal, Txr was kept switched off and 100 kHz (10 μs) baseband signals of rectangular pulses of 50% duty cycle and in magnitude steps of 10 mV to a maximum of 100 mV were AM modulated individually on Tx carrier frequency (3.2 GHz). The SI at the DA inputs is the Tx modulating signal recovered by the two receivers (Fig. 1). However, these detected pulses at the two channels had slightly different shapes, widths and magnitudes mainly because of different noise contaminations, small delays (RF phase misalignment of the two receiver mainly), non-linearities and non-exact attenuator value. The output at the DA stage was recorded using an oscilloscope for amplitude measurement and a spectrum analyser for power measurement. The purpose of the measurement was to reveal the capability of the DA in rejecting its own transceiver SI as well as the effects of SI on the dual-receiver noise level, as shown in Fig. 7. As noted earlier before the baseband detection circuits, the RF SI is already attenuated by 45.3 dB by the antenna system in Rx2 channel.

Fig. 7 shows the plots for SI rejection and SI level at the DA output. For 10 mV baseband signal, the maximum detected baseband interference signal was around 0.13 mV resulting in SI rejection of −38 dB (Fig. 7a), and for this case the SI power level recorded at the DA output was −87.1 dBm (Fig. 7b), which means the receiver noise floor has risen by 8 dBm (from the original −95.1 dBm). At the other extreme, for 100 mV baseband signal, the interference at the DA output was 0.55 mV corresponding to a SI rejection of −45.2 dB in which case the SI power level recorded was −78.8 dBm deteriorating the original noise floor by 16.3 dBm. The findings are in agreement with the fact (as alluded earlier) that the SI of an FD system is a function of the transmit power. The comparison of these two studies suggests that for deeper AM modulations the SI rejection improves as the copies of SIs received at Rx1 and Rx2 are more similar in shape (as they are less affected by the system noise etc.), but the noise level due to SI increases because of the production of the larger residue of the SI level. Therefore, depending on the level of the modulating signal in Tx (10–100 mV), the system noise and interference level (combined) vary between −87.1 and −78.8 dBm. Hence, the tangential sensitivity of the system at the DA output would vary between −79.1 and −70.8 dBm (considering signal to be 8 dBm stronger than noise and SI level combined).

Note that as Fig. 7a shows, the SI rejection improves little for baseband signals above 60 mV. Further, the overall SI rejection by the antenna system and DA is 83.3 dB (45.3 dB antenna + 38 dB DA) for 10 mV and 90.5 dB (45.3 dB + 45.2 dB) for 100 mV modulating signals (pulses).
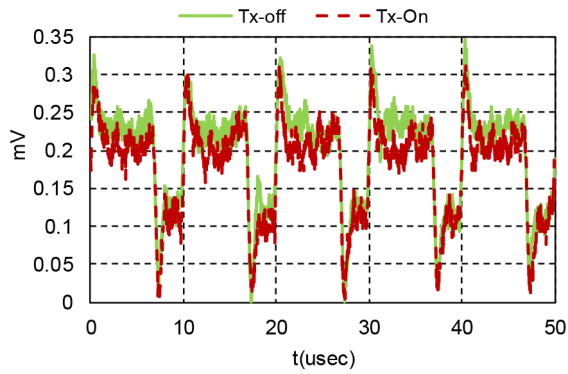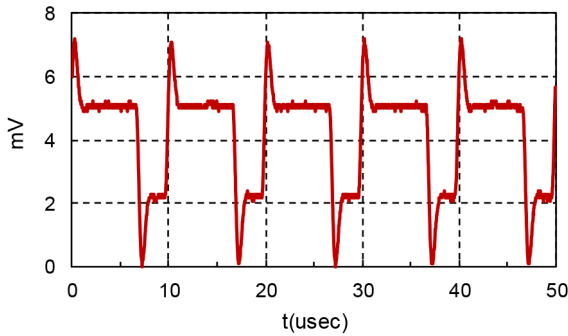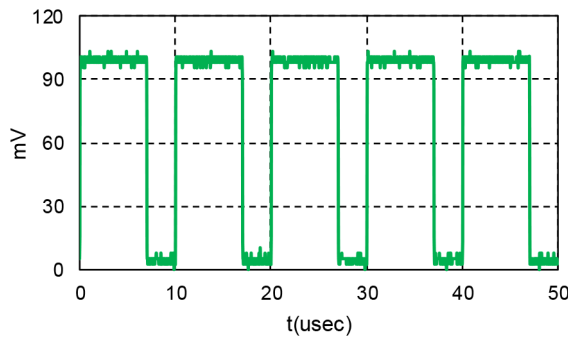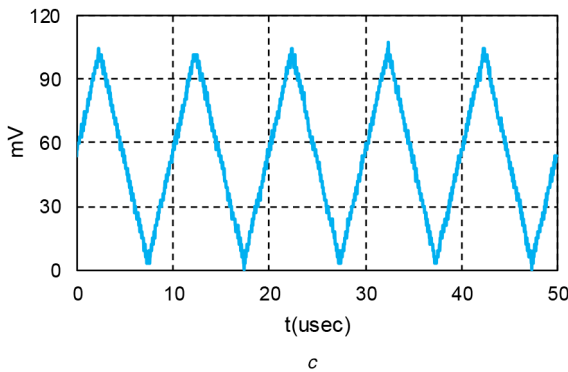
Fig. 8 *Detected baseband signal (data) with Tx on (with SI present) and with Tx off (without SI present) for 10 mV data signal amplitude*
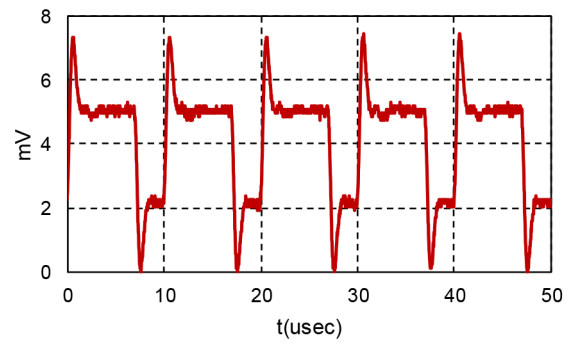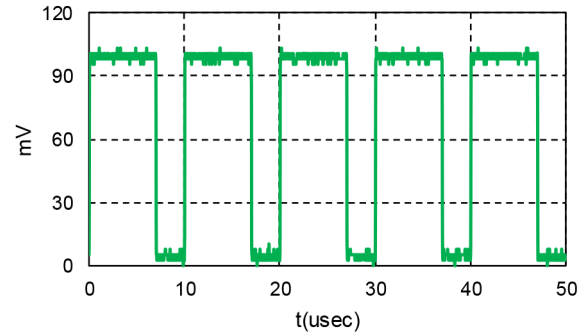

Fig. 9

(a) Time-domain baseband signal from Txr recovered after DA stage, *(b)* Transmitted baseband signal from Txr (rectangular pulses with 30% duty cycle and 100 mV amplitude), *(c)* Transmitted baseband signal from Tx (triangular pulses with 100 mV amplitude)

Fig. 10

(a) Time-domain baseband signal from Txr recovered after DA stage, *(b)* Transmitted baseband signal from Txr (rectangular pulses with 30% duty cycle and 100 mV amplitude), *(c)* Transmitted baseband signal from Tx (rectangular pulses with 50% duty cycle and 100 mV amplitude)
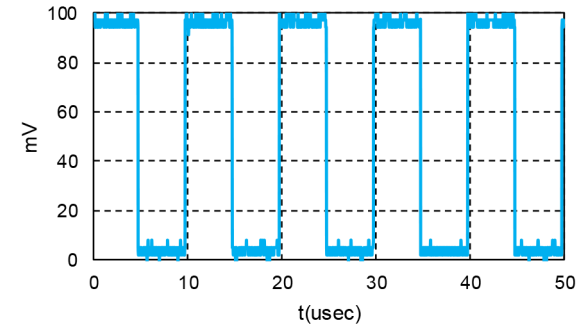
To determine the minimum required power at the dual-receiver antennas to meet the receiver sensitivity (at the DA output as mentioned earlier), both Tx and Txr were switched on while both carrying rectangular pulses of 100 kHz and amplitude of 10 mV. The Txr data (in the form of rectangular pulses) was set at 30% duty cycle for clarity of demonstration and an attenuator was implemented at the input of Txr antenna to change the transmit power. The Tx modulating pulses were set at 50% duty cycle. Data (baseband received from Txr) was found easily detectable when it produced −79.1 dBm power (sensitivity criterion stated earlier) at the DA output, in which case the RF received signal power at the outputs of Rx1 and Rx2 antennas was −63.5; −15 dBm weaker than the no-modulated RF signal measured previously at −48.5 dBm at the outputs of the antennas. Therefore, considering the gain (around 5 dB) of the receiver antennas, the sensitivity of the receiver is about −68.5 dBm. Fig. 8 shows the detected baseband signal (data) without SI being present (Tx switched off) and the same with SI present (Tx switched on) for the data signal having 10 mV in amplitude. For data (from Txr) with magnitudes above 10 mV, the power at the receiver antennas increased beyond the −68.5 dBm and reliable detection was found to be achievable. The spikes on the recovered data (Fig. 8) were found to be due to the inadequate transient response of the DA.

By using the proposed FD system, different target baseband signals were successfully recovered without using complicated circuits or algorithms. Two examples are shown in Figs. 9 and 10. In these examples the power at the input of Txr and Tx antennas were kept nearly equal (Txr = −5.8 dBm, Tx = −5.6 dBm) assuming all transmitters of equal output power. Fig. 9a shows the recovered data with 30% duty cycle and 100 mV amplitude (Fig. 9b), which was transmitted by Txr in the presence of triangular modulating signal of 100 mV amplitude (Fig. 9c) transmitted by Tx. Fig. 10a

shows the recovery of the same data (Fig. 10*b*), transmitted by Txr, in the presence of the rectangular modulating signal of 50% duty cycle and 100 mV amplitude transmitted by Tx (Fig. 10*c*).

It should be noted that the overall sensitivity of the system mentioned earlier was found to be dependent on the proper calibration of the system which effectively rests on the balancing of the interference powers detected by the two receivers at the input of the DA. In other words, the components and circuits in two receiver channels should be as matched as possible which can be achieved if the proposed FD system is to be developed on silicon using the present MIC technology. Also note that the Q2measurements were conducted in a real-time scenario along with multi-path propagations (using non-anechoic settings). The architecture of the system allows this system to be scaled and used for other frequency bands provided that a differential circuit (replacing the DA) and an antenna system with correct bandwidth and spacings between elements are made available.

3 Conclusion

The design and validation prototype of an FD system capable of recovering a target baseband signal without utilising complex circuitry or digital signal processing are presented. Therefore, it would be fit for implementation in broadband mm-wave FD transceivers where digital-to-analogue conversion at the baseband is not an option for digital SI suppression. The proposed system utilises a dual-patch three-port antenna system together with a dual receiver. The transmitting and receiving antennas are orthogonally polarised to maximise the isolation between the transmitter and receiver. The measured isolation between the transmitter and receiver antennas was found to be around 45.1 dB over a bandwidth of 60 MHz. The equalised output from the two receivers passed through a DA provided a further 36.4 dB of SI cancellation at the baseband in which case a large overall SI rejection of 81.5 dB (45.1 dB + 36.4 dB) is achievable with the system. For the demonstrated system with transmit power of −5.6 dBm and a weak modulating data of pulses of 10 mV peak, the minimum detectable AM modulated received signal was found to be about −68.5 dBm at the receiver antennas. It was shown that the proposed analogue FD system was able to recover reliably different types of baseband signals in the presence of the multipath condition.

The performance of the system is dependent on the power equalisation of SIs at the outputs of the two receivers (calling for matched components and circuits for the dual receiver) and the quality of the differential device at the outputs of the dual receiver. Future research will focus on the development of appropriate DAs and phase adjustment of the two receivers for this class of FD radios for broadband operation.

5 References

[1] Sabharwal, A., Schniter, P., Guo, D.*, et al.*: 'In-band full-duplex wireless: challenges and opportunities', *IEEE J. Sel. Areas Commun.*, 2014, **32**, (9), pp. 1637–1652

[2] Duarte, M., Dick, C., Sabharwal, A.: 'Experiment-driven characterization of full-duplex wireless systems', *IEEE Trans. Wirel. Commun.*, 2012, **11**, (12), pp. 4296–4307

[3] Bharadia, D., McMilin, E., Katti, S.: 'Full duplex radios', *SIGCOMM Comput .Commun. Rev.*, 2013, **43**, pp. 375–386

[4] Duarte, M., Sabharwal, A., Aggarwal, V.*, et al.*: 'Design and characterization of a full-duplex multiantenna system for WiFi networks', *IEEE Trans. Veh. Technol.*, 2014, **63**, (3), pp. 1160–1177

[5] Jain, M., Choi, J.I., Kim, T.*, et al.*: 'Practical, real-time, full duplex wireless'. Proc. ACM MobiCom, Los Vegas, USA, 2011, pp. 301–312

[6] Heino, M., Korpi, D., Huusari, T.*, et al.*: 'Recent advances in antenna design and interference cancellation algorithms for in-band full duplex relays', *IEEE Commun. Mag.*, 2015, **53**, (5), pp. 91–101

[7] Duarte, M., Sabharwal, A.: 'Full-duplex wireless communications using off-the-shelf radios: feasibility and first results'. Proc. Asilomar Conf. Signals, Systems Computer, CA, USA, 2010, pp. 1558–1562

[8] Everett, E., Sahai, A., Sabharwal, A.: 'Passive self-interference suppression for full-duplex infrastructure nodes', *IEEE Trans. Wirel. Commun.*, 2014, **13**, (2), pp. 680–694

[9] Nawaz, H., Tekin, I.: 'Dual port single patch antenna with high interport isolation for 2.4 GHz in-band full duplex wireless application', *Microw. Opt. Technol. Lett.*, 2016, **58**, (7), pp. 1756–1759

[10] Deo, P., Mirshekar-Syahkal, D., Zheng, G.*, et al.*: 'Broadband antenna for passive self-interference suppression in full-duplex communications'. IEEE Radio and Wireless Symp. (RWS), CA, USA, 2018, pp. 15–18

[11] Kolodziej, K.E., McMichael, J.G., Perry, B.T.: 'Multitap RF canceller for in-band full-duplex wireless communications', *IEEE Trans. Wirel. Commun.*, 2016, **15**, (6), pp. 4321–4334

[12] Zhou, J., Chuang, T.-H., Dinc, T.*, et al.*: 'Integrated wideband self-interference cancellation in the RF domain for FDD and full-duplex wireless', *IEEE J. Solid-State Circuits*, 2015, **50**, (12), pp. 3015–3031

[13] Masmoudi, A., Le-Ngoc, T.: 'Channel estimation and self-interference cancellation in full duplex communication systems', *IEEE Trans. Veh. Technol.*, 2017, **66**, (1), pp. 321–334

[14] Masmoudi, A., Le-Ngoc, T.: 'A maximum-likelihood channel estimator for self-interference cancellation in full-duplex systems', *IEEE Trans. Veh. Technol.*, 2016, **65**, (7), pp. 5122–5132

[15] Riihonen, T., Werner, S., Wichman, R.: 'Mitigation of loopback self-interference in full-duplex MIMO relays', *IEEE Trans. Signal Process.*, 2011, **59**, (12), pp. 5983–5993

[16] CST – Computer Simulation Technology GmbH. Available at www.cst.com

IET-MAP20190539